RSC Advances

ROYAL SOCIETY OF CHEMISTRY

www.rsc.org/advances

RSC Advances RSCPublishing

ARTICLE

Design, Synthesis and Biological Evaluation of Shikonin Thio-glycoside Derivatives: New Anti-Tubulin Agents

Cite this: DOI: 10.1039/x0xx00000x

Hong-Yan Lin [a], Hong-Wei Han [a], Li-Fei Bai [b], Han-Yue Qiu [a], De-Zheng Yin[c], Jin-Liang Qi [a], Xiao-Ming Wang [a,*], Hong-Wei Gu [a,*] and Yong-Hua Yang [a,*]

Received 00th January 2014,
Accepted 00th January 2014

DOI: 10.1039/x0xx00000x

www.rsc.org/

Abstract

A novel series of acetyl-*β*-*D*-thio-glycoside modified shikonin derivatives were designed and synthesized and investigated for inhibition of cell proliferation against MG63, MCF-7, B16-F10, HepG2, MDA-231, L02, VERO and MCF-10A cell lines. The biological study showed that most single, di- and tri- substituted shikonin derivatives exhibited better anti-proliferative activities against the five cancer cell lines but lower cytotoxic activity against normal cells than shikonin itself. Notably, compared to shikonin, **IIb** displayed much stronger anti-proliferative effect among them. Furthermore, the inhibition of tubulin polymerization results indicated that **IIb** showed the most potent anti-tubulin activity (IC_{50} = 4.67±0.433 μM), which was compared with shikonin (IC_{50} = 16.8±0.625 μM) and colchicine (IC_{50} = 3.83±0.424 μM). Docking simulation, confocal microscopy and western bolt results further confirmed that **IIb** can cause cell arrest in G2/M phase and induce cell apoptosis *via* binding to the active site of tubulin and inhibiting tubulin polymerization.

Keywords:

acetyl-*β*-*D*-thio-glycoside; anti-cancer; anti-tubulin; shikonin derivatives

Introduction

Microtubules are key cytoskeletal filaments which are involved in various crucial cellular processes such as cell motility, cell division, shape maintenance and vesicle transport[1, 2]. Inhibiting tubulin polymerization or interfering with microtubule disassembly will interrupt the dynamic equilibrium, leading to cell cycle arrest or apoptosis induction[3]. Due to its significant role in the cellular functions, microtubule has been a proven molecular target for cancer chemotherapeutic agents[4, 5]. Acharya *et al.* [6] reported that naphthazarin is a microtubules inhibitor in cell-free system and in A549 cells. Naphthazarin plays a role as microtubule depolymerizing agent which induces both apoptosis and autophagy in A549 lung cancer cells.

Shikonin and its derivatives are active naphthoquinone compounds that are isolated from the root of Chinese herbal medicine *Lithospermum erythrorhizon*[7], have been reported to possess numerous biological activities, such as anti-oxidant activities[8], anti-inflammatory[9], inhibiting adipogenesis[10], anti-HIV[7] and anti-cancers activities[11-13]. However, as a potential anti-cancer drugs，it is poorly soluble and believed to exert strong cytotoxic effects on normal cells[14]. Hence, a large number of researchers are dedicated to synthesizing and preparing some new and effective shikonin derivatives.

As is summarized in **Fig. 1**, based on the shikonin skeleton, compound **B**, **C** and **G** used methyl to substitute hydroxyl hydrogen atoms[14-16]; compound **E** not only replaced the phenol hydroxyl with methyl, but also completely changed the structure of its side chain to give a better anti-cancer agent, 2-hyim-DMNQ-S3317; compound **F** and **H** completely changed the side chain to give the novel shikonin derivatives[18-20]; compound **D** linked the ester group or O-glycoside to obtained functional molecules[15], [16], [21-24] and compound **I** was added to the fragments which contain amino or thiol groups derivatization of acrylshikonin[25, 26]. To sum up, by changing the chain line or replacing a number of structural elements based on the 5, 8-Dihydroxy-1, 4-naphthoquinone ring, a series of newly functional compounds can be obtained. However, most compounds among them did not resolve the toxicity against normal cells or solubility problems. Based on these, we hope to get more effective structures of shikonin derivatives.

After investigation, we found that glycoside drugs consisting of more glycoside present better solubility and play an important role in the treatment of diseases[27-29]. Su *et al.* [22] synthesized some glycoside shikonin derivatives which use O atom as linkages and confirmed that those compounds are good candidates of anti-tumor agents. In addition, He *et al.* [28] synthesized some aminoglycosides of shikonin or alkannin which improve their DNA-binding affinity. Zhao *et al.* [30] reported that the introduction of a thioether functional group at the 1'-position in the side chain of shikonin is associated with an increase in cytotoxicity. Therefore, we used different methods to obtain fifteen glycoside shikonin derivatives which used S atom as linkages. And the results indicated that all of the shikonin acetyl-*β*-*D*-thioglycosyl derivatives exhibited stronger if not the same cytotoxicity against cancer cell lines than shikonin itself and arouse considerable interest of us to further study the underlying mechanism.

Results and discussion

The synthetic routes for the novel thio-glycosyl shikonin derivatives **Ia-IIId** is outlined in **Scheme 1**. These compounds were synthesized from *β*, *β*-dimethylacrylshikonin and acetyl-*β*-*D*-thio-glycosides. The desired acetyl-*β*-*D*-thio-glycoside could be obtained by three steps (acetylating, brominating and thionation reaction[31-32]) from six kinds of glycosides. Acetyl-*β*-*D*-thio-glycoside and *β*, *β*-dimethylacrylshikonin were dissolved in ethanol to furnish the corresponding shikonin derivatives. The reaction occurred at the side chain ester group, benzene ring and quinine ring of *β*, *β*-dimethylacrylshikonin, respectively. All the target compounds were characterized by IR, ^{1}H NMR, elemental analysis and mass spectrum, which were in full accordance with their depicted structures.

All synthesized shikonin derivatives **Ia-IIId** were evaluated for their anti-proliferative activities against five cancer cell lines, human osteosarcoma cell (MG63), human breast cancer cell (MCF-7), melanoma cell (B16-F10), human hepatoma cell (HepG2), human breast cancer cell (MDA-231) and three normal cell lines, normal human liver cells (L02), African green monkey kidney cell (VERO) and normal breast cells (MCF-10A). The results are summarized in **Table 1**. A number of acetyl-*β*-*D*-thio-glycoside substituted shikonin compounds which bearing the same dithiocarbamate (DTC) moiety showed remarkable effects on anti-proliferation.

Generally speaking, all of the synthetic compounds have significant anti-proliferative effects on MG63, MCF-7, B16-F10 and MDA-231 cancer cell lines except HepG2. However, **IIb** (IC_{50}= 1.22±0.110 μM) not only showed good anti-proliferative activities against MG63, MCF-7, B16-F10 and MDA-231, but also have good inhibition effect on HepG2. For glycoside, it seems that the compounds with different glycosides exhibited slightly more potent activities in order of xylose (**b**) > glucose (**a**) > galactose (**c**), mannose (**d**) > maltose (**f**) > arabinose (**e**). Among the three compounds which contain xylose moieties (**Ib**, **IIb**, **IIIb**), **IIb** with two xyloses showed the best anti-proliferative activities; **IIIb** with three xyloses took second place and **Ib** with single xylose was the worse.

According to MTT assay results, **IIb** (IC_{50}= 1.22±0.221 μM, 2.37±0.165 μM and 1.22±0.110 μM for MG63, MCF-7 and HepG2, respectively) showed the best anti-proliferative activities against MG63, MCF-7 and HepG2 cell lines. Meanwhile, **IIIb** (IC_{50}= 3.75±0.273 μM) has the best anti-proliferative effect on B16-F10 cell line and **Ic** (IC_{50}= 4.97±0.37 μM) is the best proliferation inhibitor against MDA-231 cell line. In addition, the IC_{50} values of all the compounds against three normal cell lines, L02, VERO and MCF-10A, indicated that all of them have hardly any cytotoxicity against normal cells.

Then we performed the tubulin assembly assay to examine whether the compounds interact with tubulin and inhibit tubulin polymerization in *vitro*. As is shown in **Table 1**, **Ia**, **IIb**, and **IIIb** showed strong inhibitory effect and their 50% tubulin polymerization inhibition are 10.0±0.311 μM, 4.67±0.433 μM, and 7.57±0.742 μM, respectively. Obviously, **IIb** displayed the most potent anti-tubulin polymerization activity. These findings indicate a continuing impairment of cell division and proved **IIb** is a potent anti-tubulin agent.

For better understanding of the potency of **IIb** and guide further SAR studies, we examined the interaction of **IIb** with tubulin

(PDB code: 1SA0). All docking runs were applied the Lamarckian genetic algorithm of Auto-Dock 4.0. All the amino acid residues which had interactions with tubulin were exhibited. Because of the uncertainty of the compound structure, we conducted the docking simulation of the two structures respectively. And the interactions of **IIb** with the colchicine binding site are depicted in **Fig. 2**(A) and **2**(C). All the amino acid residues of tubulin which had interactions with **IIb** were exhibited. In the first binding model, **IIb** is nicely bound to the colchicine binding site of tubulin via four hydrogen bond with CYS 241 (distance = 2.26 Å), ASN 258 (distance = 2.07 Å), ASN 101 (distance = 2.35 Å) and LYS 254 (distance = 1.99 Å). And in the second binding mode, **IIb** can also bound to the colchicine binding site of tubulin well *via* three hydrogen bond with LYS 254 (distance = 2.36 Å), ASN 258 (distance = 2.36 Å), ASN 101 (distance = 1.96 Å) and two π bonds with LYS 352 (distance = 6.72 Å and 6.44 Å). For **Fig. 2**(B) and **2**(D), the 3D models of the interaction between **IIb** and the colchicine binding site of tubulin was depicted. The molecular docking results argue that **IIb** may be a potential anti-tubulin agent *via* binding to the colchicine binding site of tubulin and then inhibit tubulin polymerization.

To further determine the mechanism by which acetyl-*β*-*D*-thio-glycoside modified shikonin derivatives induced cell death, we assessed cell cycle distribution of HepG2 cells by flow cytometry. Treatment of HepG2 cells with **IIb** for different time could arrest cells at G2/M transition. This study further showed that treatment with **IIb** led to an obvious G2/M arrest in concentration- and time-dependent manners in HepG2 cells as shown in **Fig. 3**. Treatment of HepG2 cells with varying doses of **IIb** for 24 hours resulted in the increased accumulation of the cells in G2/M phase (**Fig. 3**(A)). Incubation of cells with 3 μM **IIb** for 24 hours caused 17.39% enrichment of cells in G2/M phase compared with the control. When the drug concentration increases to 10 μM, 26.45% cells are arrest in G2/M phase. In a time-dependent experiment, maximum accumulation of cells in the G2/M phase was observed after treatment of cells with 3 μM **IIb** for 48 hours (**Fig. 3**(B)).

We also treated HepG2 cells with varying concentrations of **IIb** and analyzed cells for changes in apoptotic markers by flow cytometer in vitro. The results are shown in **Fig. 4**(A), after treated with increasing concentrations of **IIb**, the percentage of apoptotic cell has a significant increase. Meanwhile, the time-dependent assay result which was shown in **Fig. 4**(B) indicates that cell apoptosis presents a time-dependent manner.

The preliminary results make us to speculate that **IIb** causes HepG2 cells arrest at G2/M phase and thus induces cell apoptosis possibly by inhibiting the polymerization of tubulin.

To assess the effect of drug on cell microtubules, confocal microscopy analyses on HepG2 cells was carried out. The results were shown in **Fig. 5**. After treating cells with 3 μM **IIb** for 12 hours and 24 hours, we found the morphology of cells changed obviously. In the control group, cells are round and the cytoskeleton is integrated. When treated with drug for 12 hours, cytoskeleton is affected significantly. Drug inhibited the formation of spindle, which lead to the chromosome cannot move toward the poles and finally formed multinuclear cells. After 24 hours of drug treating, we found that the entire cytoskeleton suffered serious damage; cell membranes and nucleus are deformed and eventually induce apoptosis. These results indicate that **IIb** can inhibit the formation of microtubules during mitosis of HepG2 cells, and this is in line with the molecular docking simulation results.

In order to further investigate its' effect on microtubule organization, we did an in *vitro* microtubule assembly assay. As shown in **Fig. 6**, HepG2 cells were treated with 3 μM **IIb**, 1 μM paclitaxel, and 1 μM colchicine for 24 hours, respectively. With comparison, **IIb** and colchicine caused inhibition of microtubule assembly. However, paclitaxel significantly induced promotion of tubulin polymerization. To sum up, our results demonstrate that **IIb** induced mitotic arrest and inhibited the polymerization of microtubules in HepG2 cells.

Experimental

General information and materials

The eluates were monitored using TLC. Melting points (uncorrected) were determined on a XT4MP apparatus (Taike Corp., Beijing, China). Infrared (IR) spectra were recorded on a NEXUS870 spectrometer (NICOLET Co. USA), using KBr pellet (solid). ^{1}H NMR spectra were determined on Varian Mercury-300 spectrometer at 25 °C with TMS and solvent signals allotted as internal standards, Chemical shifts are reported in ppm (d), Elemental analyses were performed on a CHN-O-Rapid instrument and were within 0.4% of the theoretical values. ESI mass spectra were obtained on a Mariner Bio-spectrometry Workstation (ESI-TOF) mass spectrometer. Reagents and solvents were commercially available. Solvents were dried and purified using standard techniques. Column chromatography was run on silica gel (200-300 meshes) from Qingdao Ocean Chemical Factory.

Paclitaxel and colchicine were purchased from Sigma-Aldrich (St. Louis, MO) and dissolved in DMSO. $MgCl_2$, EGTA, NP-40, PMSF, Aprotinin, amino caproic acid, benzamidine and Tris-HCl, pH 6.8 were purchased from Sangon (Shanghai,

China) and dissolved in PBS. *β*-tubulin antibody were purchased from Sino Biological Inc.(Beijing, China).

General procedure for Preparation of *β*, *β*-dimethylacrylshikonin

In 5 litre beaker, 1 Kg of the crushed herb *Lithospermium erythrorhizon* (100 meshes) was soaked in petroleum ether for two days. Then the residua was filtrated and washed with petroleum ether twice; the organic layer was collected and the solvent was evaporated to dryness. After that, the residue was dissolved in 200 mL of petroleum ether and was dumped into the 500 mL beaker to be slowly crystallization. Until a large number of the red powder appeared at the bottom of the beaker, we filtrated and washed residua with petroleum ether (20 mL×2). Finally, the residua was dried in the air to given red power of *β*, *β*-dimethylacrylshikonin.

General procedure for the preparation thio-glycoside (Ia-If, IIa-IIf and IIIa-IIId).

Adding *β*, *β*-dimethylacrylshikonin (1 mmol dissolved in 15 mL EtOH) to a solution of acetyl-*β*-*D*-thio-glycoside (1 mmol dissolved in 15 mL EtOH) at room temperature and the resultant mixture was stirred at room temperature for 30 minutes under a nitrogen atmosphere. Until no further changes in TLC, the reaction was stop. Removal of solvent and purification of the residue by column chromatography gave the product. Purification by silica gel chromatography (ethylacetate: petroleum ether *V/V* = 1:2) afforded the shikonin thio-glycoside. The disubstituted method is similar to the above one, while just changing thio-glycoside moles to 2 mmol and reaction system's temperature to 40 °C, then the corresponding disubstituted compounds can be obtained. The tri-substituted product can be obtained by changing thio-glycoside moles to 3 mmol, reaction system's temperature to 60 °C and reaction time to 1 hour, then separated the target compounds by column chromatography solvent ratio (ethylacetate: petroleum ether *V/V*= 1:1).

2, 3, 4, 6-tetra-*O*-acetyl-1-thio-*β*-*D*-glucopyranosyl shikonin (Ia)

Red powder, yield 20%; mp: 97.5-99.7 °C; IR (KBr) 3440, 2959, 2926, 1755, 1652, 1610, 1455, 1228, 1039 cm^{-1}; ^1H NMR (300 MHz, $CDCl_3$) *δ*: 1.61(s, 3H), 1.68(s, 3H), 2.02(s, 9H), 2.05(s, 3H), 2.59(s, 2H), 3.62-3.65 (m, 1H), 4.02(d, *J* = 11 Hz, 1H), 4.40(t, *J* = 7 Hz, 1H), 4.478(d, *J* = 10 Hz, 1H), 4.55(t, *J* = 7 Hz, 1H), 5.00-5.11 (m, 3H), 5.17-5.21 (m, 1H), 7.12(s, 1H), 7.22(s, 2H), 12.45 (s, 1H), 12.66(s, 1H); ESI-TOF, calcd for $C_{30}H_{34}O_{13}S$ ($[M+Na]^+$) 657.1720, found 657.1745. Anal. Calcd for $C_{30}H_{34}O_{13}S$: C, 56.77; H, 5.40; O, 32.77; S, 5.05. Found: C, 69.31; H, 6.71; O, 23.94, S, 5.01.

2, 3, 4-tri-*O*-acetyl-1-thio-*β*-*D*-xylopyranosyl shikonin(Ib)

Red powder, yield 25%; mp: 86.3-88.7 °C; IR (KBr) 3444, 2925, 1755, 1608, 1572, 1435, 1372, 1223, 1053cm^{-1}; ^1H NMR (300 MHz, $CDCl_3$) *δ*: 1.60(s, 3H), 1.67(s, 3H), 2.04(s, 9H), 2.56-2.62(m, 2H), 3.61-3.64(m, 1H), 4.38-4.47(m, 1H), 4.57(d, *J* = 8 Hz,1H), 4.84(t, *J* = 8 Hz, 1H), 4.87-4.91(m, 1H), 4.96(t, *J* = 8 Hz, 1H), 5.06(s, 1H), 5.09-5.12(m, 1H), 7.04(s, 1H), 7.22(s, 2H), 12.45(s, 1H), 12.62(s, 1H); ESI-TOF, calcd for $C_{27}H_{30}O_{11}S$ ($[M+Na]^+$) 585.1509, found 585.1573. Anal. Calcd for $C_{27}H_{30}O_{11}S$: C, 57.64; H, 5.37; O, 31.28; S, 5.70. Found: C, 56.89; H, 6.01; O, 31.94; S, 5.75.

2, 3, 4, 6-tetra-O-acetyl-1-thio-β-D-galactopyranosyl shikonin (Ic)

Red powder, yield 18%; mp: 95.0-98.2 °C; IR (KBr) 3436, 2927, 1752, 1610, 1570, 1455, 1369, 1225, 1055cm^{-1}; ^1H NMR (300 MHz, $CDCl_3$) *δ*: 1.62(s, 3H), 1.67(s, 3H), 2.00(s, 9H), 2.01(s, 3H), 2.52(s, 2H), 3.60-3.62 (m, 1H), 4.05(d, *J* = 10.5 Hz, 1H), 4.37(t, *J* = 6.0 Hz, 1H), 4.47 (d, *J* = 9.5 Hz, 1H), 4.58(t, *J* = 7 Hz, 1H), 4.95-5.08 (m, 3H), 5.13-5.19 (m, 1H), 7.10(s, 1H), 7.18(s, 2H), 12.38 (s, 1H), 12.63(s, 1H)；ESI-TOF, calcd for $C_{30}H_{34}O_{13}S$ ($[M+Na]^+$) 657.1720, found 657.1764. Anal. Calcd for $C_{30}H_{34}O_{13}S$: C, 56.77; H, 5.40; O, 32.77; S, 5.05. Found: C, 69.31; H, 6.71; O, 23.94, S, 5.01.

2, 3, 4, 6-tetra-*O*-acetyl-1-thio-*β*-*D*-mannopyranosyl shikonin (Id)

Red powder, yield 16%; mp: 96.3-99.6 °C; IR (KBr) 3447, 2969, 1753, 1614, 1565, 1437, 1372, 1225, 1053, 975cm^{-1}; ^1H NMR (300 MHz, $CDCl_3$) *δ*: 1.58(s, 3H), 1.65(s, 3H), 2.02(s, 3H), 2.03(s, 3H), 2.04 (s, 3H), 2.05(s, 3H), 2.55(s, 2H), 3.60-3.62 (m, 1H), 4.00(d, *J* = 10 Hz, 1H), 4.35(t, *J* = 7.5 Hz, 1H), 4.48(d, *J* = 10.5 Hz, 1H), 4.58(t, *J* = 7.5 Hz, 1H), 5.05-5.13 (m, 3H), 5.20-5.25 (m, 1H), 7.14(s, 1H), 7.25(s, 2H), 12.48 (s, 1H), 12.69(s, 1H)； ESI-TOF, calcd for $C_{30}H_{34}O_{13}S$ ($[M+Na]^+$) 657.1720, found 657.1756. Anal. Calcd for $C_{30}H_{34}O_{13}S$: C, 56.77; H, 5.40; O, 32.77; S, 5.05. Found: C, 69.31; H, 6.71; O, 23.94, S, 5.01.

2, 3, 4-tri-*O*-acetyl-1-thio-*β*-*D*-arabinopyranosyl shikonin(Ie)

Red powder, yield 11%; mp: 85.7-87.5 °C; IR (KBr) 3446, 2926, 2857, 1751, 1610, 1572, 1454, 1435, 1372, 1221, 1054cm^{-1}; ^1H NMR (300 MHz, $CDCl_3$) *δ*: 1.55(s, 3H), 1.65(s, 3H), 2.03(s, 3H), 2.04(s, 3H), 2.05(s, 3H), 2.50-2.60(m, 2H), 3.60-3.61 (m, 1H), 4.40(d, *J* = 8.5 Hz, 1H), 4.57(d, *J* = 7.5

Hz,1H), 4.82(t, *J* = 7.5Hz, 1H), 4.85-4.90(m, 1H), 4.95(t, *J* = 8 Hz, 1H), 5.06(s, 1H), 5.08-5.10(m, 1H), 7.04(s, 1H), 7.22(s, 2H), 12.40(s, 1H), 12.60(s, 1H) ; ESI-TOF, calcd for $C_{27}H_{30}O_{11}S$ ([M+Na]$^+$) 585.1509, found 585.1578. Anal. Calcd for $C_{27}H_{30}O_{11}S$: C, 57.64; H, 5.37; O, 31.28; S, 5.70. Found: C, 56.89; H, 6.01; O, 31.94; S, 5.75.

2, 3, 6-tri-*O*-acetyl-(2, 3, 4, 6-tetra-*O*-acetyl-*α*-*D*-glucopyranosyl-)-1-thio- *β*-*D*- glucopyranosyl shikonin(If)

Red powder, yield 19%; mp: 103.1-105.6 °C; IR (KBr) 3441, 2938, 1753, 1683, 1652, 1611, 1436, 1370, 1229, 1050cm^{-1}; ^{1}H NMR (300 MHz, $CDCl_3$) *δ*: 1.59(s, 3H) , 1.66(d, *J* = 7 Hz, 3H), 1.99-2.05(m, 15H) , 2.10(d, *J* = 6 Hz, 6H), 2.58(s, 2H) , 3.53-3.61(m, 1H), 3.92(t, *J* = 8.5 Hz, 2H) , 3.96-4.01 (m, 1H), 4.05(t, *J* = 22 Hz, 1H), 4.16-4.26(m, 1H), 4.32-4.40(m, 1H), 4.50(t, *J* = 10.5 Hz, 1H), 4.69-4.76(m, 1H), 4.82-4.86(m, 1H), 4.90(t, *J* = 10 Hz, 1H), 5.04(t, *J* = 9.5 Hz, 1H), 5.23(t, *J* = 9 Hz, 1H), 5.32(t, *J* = 10.5 Hz, 1H), 5.37(s, 1H), 7,08(d, *J* = 35 Hz, 1H), 7.23(s, 2H), 12.46(s, 1H), 12.64(s, 1H); ESI-TOF, calcd for $C_{42}H_{50}O_{21}S$ ([M+Na]$^+$) 945.2565, found 945.2652. Anal. Calcd for $C_{42}H_{50}O_{21}S$: C, 54.66; H, 5.46; O, 36.41; S, 3.47. Found: C, 53.55; H, 6.03; O, 36.94; S, 3.51.

2, 3, 4, 6-tetra-*O*-acetyl-1, 6' or 7'-di-thio-*β*-*D*-glucopyranosyl disubstituted shikonin (IIa)

Red powder, yield 15%; mp: 125.0-127.2 °C; IR (KBr) 3458, 2914, 1720, 1613, 1565, 1430, 1368, 1225, 1058cm^{-1}; ^{1}H NMR (300 MHz, $CDCl_3$) *δ*: 1.57(s, 3H), 1.66(s, 3H), 2.01(d, *J* = 1.8 Hz, 6H), 2.04(s, 3H), 2.06(s, 3H), 2.10(t, *J* = 1.8 Hz, 9H), 2.18(s, 3H), 2.62(t, *J* = 4.5 Hz, 2H), 3.57-3.60(m, 1H), 3.95(t, *J* = 5.1 Hz, 1H), 4.05(d, *J* = 7.2 Hz, 1H), 4.15-4.20(m, 2H), 4.27(d, *J* = 6.9 Hz, 1H), 4.35(d, *J* = 6 Hz, 1H), 4.67(t, *J* = 4.2 Hz, 1H), 4.99-5.06(m, 4H), 5.12-5.16(m, 2H), 5.30(t, *J* = 5.7 Hz, 1H), 5.36(t, *J* = 5.55 Hz, 1H), 6.99(s, 1H), 7.39(s, 1H), 12.50(s, 1H), 12.72(s, 1H); ESI-TOF, calcd for $C_{44}H_{52}O_{22}S_2$ ([M+Na]$^+$) 1019.2392, found 1019.2413. Anal. Calcd for $C_{44}H_{52}O_{22}S_2$: C, 53.01; H, 5.26; O, 35.30; S, 6.43. Found: C, 52.54; H, 5.76; O, 35.87; S, 6.54.

2, 3, 4-tri-*O*-acetyl-1, 6' or 7'-di-thio-*β*-*D*-xylopyranosyl disubstituted shikonin (IIb)

Red powder, yield, 9%; mp: 103.4-106.5 °C; IR (KBr) 3438, 2927, 1742, 1602, 1564, 1495, 1229, 1037cm^{-1}; ^{1}H NMR (300 MHz, $CDCl_3$) *δ*: 1.59(s, 3H), 1.67(s, 3H), 2.08-2.05(m, 9H), 2.15-2.11(m, 9H), 2.61(s, 2H), 3.23-3.34(m, 1H), 3.23-3.34(m, 1H), 3.63-3.70(m, 1H), 3.89-4.12(m, 1H), 4.19-4.24(m, 1H), 4.34-4.38(m, 1H), 4.47(t, *J* = 6.75 Hz, 1H), 4.60(s, 1H), 4.81-4.86 (m, 1H), 4.92-4.99(m, 2H), 5.06-5.14(m, 4H), 5.25(t, *J* = 9 Hz, 2H), 7.02(s, 1H), 7.12 (s, 1H), 12.23(s, 1H), 12.76(s, 1H); ESI-TOF, calcd for $C_{38}H_{44}O_{18}S_2$ ([M+Na]$^+$) 875.1969, found 875.1997. Anal. Calcd for $C_{38}H_{44}O_{18}S_2$: C, 53.51; H, 5.20; O, 33.77; S, 7.52. Found: C, 52.54; H, 5.76; O, 33.87; S, 7.54.

2, 3, 4, 6-tetra-*O*-acetyl-1, 6' or 7'-di-thio-*β*-*D*-galactopyranosyl disubstituted shikonin (IIc)

Red powder, yield, 11%; mp: 115.0-118.9 °C; IR (KBr) 3437, 2918, 1738, 1602, 1558, 1431, 1362, 1218, 1039 cm^{-1}; ^{1}H NMR (300 MHz, $CDCl_3$) *δ*: 1.61(s, 3H), 1.65(s, 3H), 1.95-2.26(m, 24H), 2.60-2.65(m, 2H), 3.98-4.22(m, 6H), 4.48(s, 1H), 4.81(s, 1H), 4.91-5.08(m, 1H), 5.12-5.19(m, 1H), 5.36-5.56(m, 4H), 6.22(s, 1H), 6.98 (s, 1H), 12.24 (s, 1H), 12.76(s, 1H); ESI-TOF, calcd for $C_{44}H_{52}O_{22}S_2$ ([M+Na]$^+$) 1019.2392, found 1019.2415. Anal. Calcd for $C_{44}H_{52}O_{22}S_2$: C, 53.01; H, 5.26; O, 35.30; S, 6.43. Found: C, 52.54; H, 5.76; O, 35.87; S, 6.54.

2, 3, 4, 6-tetra-*O*-acetyl-1, 6' or 7'-di-thio-*β*-*D*-mannopyranosyl disubstituted shikonin (IId)

Red powder, yield, 20%; mp: 116.5-119.1 °C; IR (KBr) 3435, 2936, 1755, 1683, 1528, 1475, 1325, 1230, 1063, 980cm^{-1}; ^{1}H NMR (300 MHz, $CDCl_3$) *δ*: 1.61(s, 6H), 1.96(s, 3H), 2.04(d, *J* = 18 Hz, 6H), 2.11(d, *J* = 9 Hz, 6H), 2.17(t, *J* = 8 Hz, 6H), 2.26(s, 3H), 2.66(s, 2H), 3.47-3.61(m, 1H), 3.92(d, *J* = 17.25 Hz, 1H), 4.03-4.27(m, 4H), 4.45-4.59(m, 1H), 4.94-5.05(m, 2H), 5.16(d, *J* = 8 Hz, 2H), 5.21(t, *J* = 10.5 Hz, 1H), 5.29(t, *J* = 5 Hz, 1H), 5.38(d, *J* = 10.3 Hz, 1H), 5.67(s, 1H), 6.96(s, 1H), 7.34(s, 1H), 12.15(s, 1H), 12.68(s, 1H); ESI-TOF, calcd for $C_{44}H_{52}O_{22}S_2$ ([M+Na]$^+$) 1019.2393, found 1019.2415. Anal. Calcd for $C_{44}H_{52}O_{22}S_2$: C, 53.01; H, 5.26; O, 35.30; S, 6.43. Found: C, 52.54; H, 5.76; O, 35.87; S, 6.54.

2, 3, 4-tri-*O*-acetyl-1, 6' or 7'-di-thio-*β*-*D*-arabinopyranosyl disubstituted shikonin (IIe)

Red powder, yield, 21%; mp: 108.9-109.6 °C; IR (KBr) 3439, 2913, 2848, 1746, 1607, 1537, 1389, 1368, 12111, 1048cm^{-1}; ^{1}H NMR (300 MHz, $CDCl_3$) *δ*: 1.61(s, 3H), 1.68(s, 3H), 2.04(d, *J* = 4.5 Hz, 3H), 2.08(d, *J* = 12.5 Hz, 6H), 2.14(d, *J* = 3 Hz, 9H), 2.20(t, *J* = 11.25 Hz, 3H), 2.54-2.73(m, 2H), 3.75(d, *J* = 12.5 Hz, 1H), 3.84(t, *J* = 15.25 Hz, 1H), 4.18-4.22(m, 1H), 4.38-4.45(m, 1H), 4.99-5.10(m, 2H), 5.17(t, *J* = 12 Hz, 1H), 5.21-5.25(m, 2H), 5.35(d, *J* = 12.5 Hz, 1H), 5.39(d, *J* = 9.5 Hz, 2H), 5.45-5.52(m, 2H), 6.14(d, *J* = 5 Hz, 1H), 7.12(s, 1H), 7.21(s, 1H), 12.20(s, 1H), 12.76(s, 1H); ESI-TOF, calcd for $C_{38}H_{44}O_{18}S_2$ ([M+Na]$^+$) 875.1969, found 875.1996. Anal. Calcd for $C_{38}H_{44}O_{18}S_2$: C, 53.51; H, 5.20; O, 33.77; S, 7.52. Found: C, 52.54; H, 5.76; O, 33.87; S, 7.54.

2, 3, 6-tri-*O*-acetyl-(2, 3, 4, 6-tetra-*O*-acetyl-*α*-*D*-glucopyranosyl-)-1,6' or 7'-di-thio-*β*-*D*- glucopyranosyl disubstituted shikonin (IIf)

Red powder, yield, 18%; mp: 125.6.4-127.1 °C; IR (KBr) 3448, 2927, 1749, 1675, 1628, 1427, 1355, 1224, 1045cm^{-1}; ^{1}H NMR (300 MHz, $CDCl_3$) *δ*: 1.55(s, 3H), 1.64(s, 3H), 1.98-2.21(m, 42H), 2.60(d, *J* = 6.5 Hz, 2H), 3.54-3.79 (m, 2H), 3.93-4.11 (m, 8H), 4.14-4.29 (m, 4H), 4.36-4.44(m, 2H), 4.55-4.69(m, 2H), 4.83-4.91(m, 3H), 4.97-5.17(m, 5H), 5.29-5.46(m, 6H), 7.00(s, 1H), 7.36(s, 1H), 12.17(s, 1H), 12.69(s, 1H); ESI-TOF, calcd for $C_{68}H_{84}O_{38}S_2$ ([M+Na]$^+$) 1595.4082, found 1595.4123. Anal. Calcd for $C_{68}H_{84}O_{38}S_2$: C, 51.91; H, 5.38; O, 38.64; S, 4.08. Found: C, 50.87; H, 6.02; O, 38.87; S, 4.54.

2, 3, 4, 6-tetra-*O*-acetyl-1, 3, 6' or 7'-tetra-thio-*β*-*D*-glucopyranosyl trisubstituted shikonin (IIIa)

Red powder, yield, 26%; mp: 178.7-180.6 °C; IR (KBr) 3559, 2932, 2917, 1789, 1667, 1635, 1425, 1217, 1038, 927cm^{-1}; ^{1}H NMR(300 MHz, $CDCl_3$) *δ*: 1.59(s, 3H), 1.66(s, 3H), 1.98-2.07(m, 30H), 2.13(s, 6H), 2.61(s, 2H), 3.59-3.62(m, 4H), 3.76-3.98 (m, 3H), 4.11-4.41(m, 5H), 5.03-5.10(m, 3H), 5.28-5.43(m, 5H), 5.56-5.81(m, 3H), 7.37(s, 1H), 12.58(s, 1H), 13.23(s, 1H); ESI-TOF, calcd for $C_{58}H_{70}O_{31}S_3$ ([M+Na]$^+$) 1381.3063, found 1381.3198. Anal. Calcd for $C_{58}H_{70}O_{31}S_3$: C, 51.25; H, 5.19; O, 36.49; S, 7.08. Found: C, 50.69; H, 5.76; O, 36.87; S, 7.54.

2, 3, 4-tri-*O*-acetyl-1, 3, 6' or 7'-tetra-thio-*β*-*D*-xylopyranosyl trisubstituted shikonin (IIIb)

Red powder, yield, 28%; mp: 148.7-150.5 °C; IR (KBr) 3537, 2984, 2938, 1746, 1628, 1610, 1408, 1224, 1013, 910cm^{-1}; ^{1}H NMR (300 MHz, $CDCl_3$) *δ*: 1.58(s, 3H), 1.65(s, 3H), 2.04-2.09(m, 27H), 2.18(s, 2H), 2.58-2.67(m, 1H), 3.27-3.37(m, 2H), 3.73-3.83(m, 3H), 3.97-4.29(m, 2H), 4.44-4.50(m, 3H), 4.56-4.67(m, 1H), 4.83-5.03(m, 3H), 5.09-5.29(m, 2H), 5.48-5.86(m, 3H), 7.34(s,1H), 12.59(s, 1H), 13.16(s, 1H); ESI-TOF, calcd for $C_{49}H_{58}O_{25}S_3$ ([M+Na]$^+$) 1165.2429, found 1165.3647. Anal. Calcd for $C_{49}H_{58}O_{25}S_3$: C, 51.48; H, 5.11; O, 34.99; S, 8.41. Found: C, 50.69; H, 5.56; O, 35.27; S, 8.54.

2, 3, 4, 6-tetra-*O*-acetyl-1, 3, 6' or 7'-tetra-thio-*β*-*D*-mannopyranosyl trisubstituted shikonin (IIId)

Red powder, yield, 19%; mp: 174.6-176.8 °C. IR (KBr) 3528, 2937, 2910, 1737, 1618, 1604, 1423, 1227, 1022, 929cm^{-1}; ^{1}H NMR (300 MHz, $CDCl_3$) *δ*: 1.54(s, 3H), 1.62(s, 3H), 1.91-2.08(m, 30H), 2.13(s, 6H), 2.58(s, 2H), 3.59-3.76(m, 3H), 3.98-4.09(m, 4H), 4.11-4.26(m, 3H), 4.41-5.03(m, 3H), 5.17-5.30(m, 6H), 5.48-5.85(s, 4H), 7.37(s, 1H), 12.58(s, 1H), 13.23(s, 1H); ESI-TOF, calcd for $C_{58}H_{70}O_{31}S_3$ ([M+Na]$^+$) 1381.3063, found 1381.3276. Anal. Calcd for $C_{58}H_{70}O_{31}S_3$: C, 51.25; H, 5.19; O, 36.49; S, 7.08. Found: C, 50.69; H, 5.76; O, 36.87; S, 7.54.

Cell lines and culture conditions

The cell lines used in this study were following: MG63, MCF-7, B16-F10, HepG2, MDA-231, L02, VERO and MCF-10A were obtained from State Key Laboratory of Pharmaceutical Biotechnology, Nanjing University. MG63, MCF-7 and B16-F10 cell lines were maintained in Dulbecco's modified Eagle's medium (DMEM) with L-glutamine; L02, VERO and MCF-10A cell lines were maintained in DMEM (High Glucose) Mixture; MDA-231 cell line was maintained in L15 medium and all of the cell lines were supplemented with 10% fetal bovine serum (FBS) at 37 °C in a humidified atmosphere containing 5% CO_2.

Anti-proliferation assay

The anti-proliferative activity of the prepared compounds against five cancer cell lines, MG63, MCF-7, B16-F10, HepG2 and MDA-231 and three normal cell lines, L02, VERO and MCF-10A were evaluated as described elsewhere with some modifications. Target tumor cell lines were grown to log phase in DMEM medium supplemented with 10% fetal bovine serum. After diluting to 2×10^4 cells mL^{-1} with the complete medium, 100 μL of the obtained cell suspension was added to each well of 96-well culture plates and then allowed to adhere for 12 hours at 37 °C, 5% CO_2 atmosphere. Tested samples at pre-set concentrations (0.1 μM, 1 μM, 10 μM, 100 μM) were added to 96 wells with shikonin as positive reference.

After 24 hours exposure period, 20 μL of PBS containing 2.5 mg mL^{-1} of MTT (3-(4, 5-dimethylthiazol-2-yl)-2, 5-diphenyltetrazolium bromide)) was added to each well. Plates were then incubated for further 4 hours, and then were centrifuged (1500 rpm at 4 °C for 10 minutes) to remove supernatant. 150 μL of DMSO was added to each well for coloration. The plates were shaken vigorously to ensure complete solubilization for 10 minutes at room temperature. The absorbance was measured and recorded on an ELISA reader (ELx800, BioTek, USA) at a test wavelength of 570 nm. In all experiments three replicate wells were used for each drug concentration. Each assay was carried out at least three times. The results are summarized in **Table1**.

Effects on tubulin polymerization

To evaluate the effect of the compounds on tubulin assembly *in vitro*, varying concentrations of **IIb** were pre-incubated with tubulin (10 μM) in glutamate buffer at 30 °C and then cooled to

0 °C. After addition of GTP, the mixtures were transferred to 0 °C cuvettes in a recording spectrophotometer and warmed-up to 30 °C and the assembly of tubulin was observed turbid metrically. The IC_{50} was defined as the compound concentration that inhibited the extent of assembly by 50% after 20 minutes incubation.

Cell-Cycle Distribution by Flow Cytometry

HepG2 cells were plated in 6-well plates (5.0×10^3 cells/well) and incubated at 37 °C for 24 hours. Exponentially growing cells were then incubated with the **IIb** at 3 μM and 10 μM. And in the time-dependent assays, exponentially growing cells were incubated with 3 μM **IIb** at 37 °C for 12 hours, 24 hours and 48 hours. Untreated cells (control) or cells treated with the compounds solvent (DMSO) were included. DMSO was used at the highest concentration used in the experiments. After then, cells were centrifuged and fixed in 70% ethanol at 4 °C for at least 12 hours and subsequently resuspended in PBS containing 0.1 mg mL^{-1} RNase A and 5 μg mL^{-1} propidium iodide (PI). Cellular DNA content, for cell cycle distribution analysis, was measured by flow cytometry using FACNcan cytofluorometer (PT. Madagasi Brosa Inc. JI. Batang Hari NO.73, Propinsi Sumatera Utara, Indonesia) plotting 10,000 events per sample. The percentage of cells in the G1, S and G2/M phases of the cell cycle and the percentage of cells in the sub-G1 peak were determined using the Flowjo 7.6.1 software after cell debris exclusion.

Flow Cytometric Analysis of Apoptosis

For Annexin V/PI assays, HepG2 cells were stained with Annexin V-FITC and PI and then monitored for apoptosis by flow cytometry. Briefly, 5×10^3 cells were seeded in 6-well plates for 24 hours and then were treated with **IIb** (0-3 μM) for 0-48 hours. Then cells were collected and washed twice with PBS and stained with 5 μL of Annexin V-FITC and 2.5 μL of PI (5 μg mL^{-1}) in 1× binding buffer (10mM HEPES, pH 7.4, 140 mM NaOH, 2.5 mM $CaCl_2$) for 30 minutes at room temperature in the dark. Apoptotic cells were quantified using a FACScan cytofluorometer (PT. Madagasi Brosa Inc. Jl. Batang Hari No. 73, Propinsi Sumatera Utara, Indonesia.). Statistical analysis was done using Flowjo 7.6.1 software.
Both early apoptotic (AnnexinV-positive, PI-negative) and late apoptotic (double positive of Annexin V and PI) cells were detected.

Confocal microscopy assay

HepG2 cells were grown on round cover slips to 70% confluence and incubated with 3 μM of **IIb** for 12 hours and 24 hours, respectively. After incubating, cells were washed with PBS three times and fixed with 4% paraformaldehyde for 20 minutes, permeabilized with 1% TritonX-100 for another 10 minutes. Then, the cells were blocked with 5% BSA for 1 hour. Subsequently, the cells were washed once with PBS, and incubated with anti-tubulin antibody (1: 500, Cytoskeleton, Inc.) in 5% BSA overnight at 4 °C. After being washed with 0.5% TritonX-100 (incubate for 5 minutes), each coverslip was added 200 μL of rhodamine-conjugated anti-sheep antibody (1: 500, Cytoskeleton, Inc.) in 5% BSA and incubated for 1 hour at room temperature followed by DAPI (5 ng mL^{-1}). Cells were then observed under an Olympus confocal microscope and data was analyzed using FV-10-ASW 1.7 viewer.

***In vitro* microtubule assembly assay**

We used an established method to measure soluble (depolymerized) and assembled (polymerized) tubulin[33]. HepG2 cells (5×10^7/flask) were seeded into the 75-T flask. Cells were exposed to paclitaxel (1 μM), colchicine (1 μM), and **IIb** (3 μM) for 24 hours. After treatment, cells were collected and washed twice with PBS then lysed at 37 °C for 5 miniutes with 50 μL of hypotonic buffer (1 mM $MgCl_2$, 2 mM EGTA, 0.5% NP-40, 2 mM PMSF, 200 units ml^{-1} aprotinin, 5 mM amino caproic acid, 1 mM benzamidine, and 20 mM Tris-HCl, pH 6.8). The cell lysates were centrifuged at 13,000 rpm for 10 minutes at 25 °C. The supernatants containing soluble (cytosolic) tubulin were separated from the pellets containing polymerized (cytoskeletal) tubulin. The pellets were resuspended in 100 μL of hypotonic buffer, sonicated on ice, mixed with 5×sample buffer, and heated for 5 minutes at 100 °C. Equal amounts of the two fractions were partitioned by SDS-polyacrylamide gel electrophoresis. Immunoblots were probed with β-tubulin monoclonal antibody and secondary HRP-conjugated antibody. The blots were developed by using an ECL kit and Kodak Bio-MAX MR film (Eastman Kodak, Rochester, NY). All results are from three independent experiments.

Docking simulations

Molecular docking of **IIb** into the 3D X-ray structure of tubulin (PDB code: 1SA0) was carried out using the Auto-Dock software (version 4.0) as implemented through the graphic user interface Auto-Dock Tool Kit (ADT 1. 4.6)[34].
The graphical user interface ADT was employed to set up the enzymes: all hydrogens were added, Gasteiger charges were calculated and nonpolar hydrogens were merged to carbon atoms. For macromolecules, generated pdbqt files were saved.

The 3D structures of ligand molecules were built, optimized (PM3) level, and saved in Mol2 format with the aid of the molecular modeling program SPARTAN (Wavefunction Inc.). These partial charges of Mol2 files were further modified by using the ADT package (version 1.4.6) so that the charges of the nonpolar hydrogens atoms assigned to the atom to which the hydrogen was attached. The resulting files were saved as pdbqt files.

Auto-Dock software (version 4.0) was employed for all docking calculations. The AUTODOCKTOOLS program was used to generate the docking input files. In all docking a grid box size of 42×45×43 points in x, y, and z directions was built, the maps were center located (115.574, 89.495, 7.664) in the catalytic site of the protein. A grid spacing of 0.375 Å (approximately one fourth of the lengths of carbon-carbon covalent bond) and a distances dependent function of the dielectric constant were used for the calculation of the energetic map. Ten runs were generated by using Lamarckian genetic algorithm searches. Default settings were used with an initial population of 50 randomly placed individuals, a maximum number of 2.5×10^6 energy evaluations, and a maximum number of 2.7×10^4 generations. A mutation rate of 0.02 and a crossover rate of 0.8 were chosen. Results differing by less than 0.5 Å in positional root-mean-square deviation (RMSD) were clustered together and the results of the most favorable free energy of binding were selected as the resultant complex structures.

Abbreviations

IR, infrared spectroscopy; NMR, nuclear magnetic resonance spectrum; TLC, thin layer chromatography; TMS, tetramethylsilane; DMSO, dimethyl sulfoxide; EGTA, ethylenebis(oxyethylenenitrilo)tetraacetic acid; PMSF, phenylmethane sulfonyl fluoride; PBS, phosphate-buffered saline; DAPI, 4',6-diamidino-2-phenylindole; BSA, bovine serum albumin.

Conclusion

In our present work, a series of novel anti-tubulin polymerization agents (**Ia-IIId**) containing shikonin skeleton and acetyl-*β*-*D*-thio-glycoside moieties were synthesized and their biological activities were also evaluated. Among them, **IIb** with two xylose moieties exhibits potent anti-proliferating effect against HepG2 cell line (IC_{50}=1.22±0.110 μM), being comparable with shikonin (IC_{50}=2.73±0.286 μM) and showed lower cytotoxity against normal cells. The docking simulation and flow cytometry results demonstrated that **IIb** can bind to the colchicine binding site of tubulin and cause HepG2 cells arrest in G2/M phase then induce cell apoptosis. Confocal microscopy assay and western blot results further confirmed that **IIb** can really inhibit tubulin polymerization. These findings prompt us to consider it as a potent anti-cancer agent.

Acknowledgements

The authors are grateful to the National Natural Science Foundation of China (NSFC) (Nos.31071082, 31170275, 31171161), the Program for Changjiang Scholars and Innovative Research Team in University (IRT1020), the Project of New Century Excellent Talents in University (NECT-11-0234) and the Natural Science Foundations of the Jiangsu (BK2011414).

Notes and references

[a] *State Key Laboratory of Pharmaceutical Biotechnology, Nanjing University, Nanjing 210093, P. R. China*

[b] *School of Life Sciences and Chemistry, Jiangsu Second Normal University, Nanjing 210093, P. R. China*

[c] *Kuang Yaming Honors School, Nanjing University, Nanjing 210093, P. R. China*

*Corresponding Author.
Tel: +86-25-83594374; Fax: +86-25-83594374
E-mail: Wangxm07@nju.edu.cn and Yangyh@nju.edu.cn

[1] M. Gatti, E. Bucciarelli and R. Lattao, *Experi. Cell Res.*, 2012, **12**, 1375-1380.

[2] P. G. Christopher and R. M. Antonina, *Cytoskeleton*, 2012, **69**, 442-463.

[3] Y. Luo, K. M. Qiu, X. Lu, K. Liu, J. Fu and H. L. Zhu, *Bioorg*. *Med*. *Chem*., 2011, **19**, 4730-4738.

[4] Y. Qian, H. J. Zhang, P. C. Lv and H. L. Zhu, *Bioorg*. *Med*. *Chem*., 2010, **18**, 8218-8225.

[5] M. A. Jordan and L. Wilson, *Nat*. *Rev. Cancer*, 2004, **4**, 253-265.

[6] B. R. Acharya, S. Bhattacharyya, D. Choudhury and G. Chakrabarti. *Apoptosis*, 2011, **16**, 924-939.

[7] X. Chen, L. Yang, N. Zhang, J. A. Turpin, R. W. Buckheit, C. Osterling, J. J. Oppenheim and O. M. Z. Howard, *Antimicrob*. *Agents Ch*., 2003, **47**, 2810-2816.

[8] Z. H. Wang, T. Liu, L. Gan, T. Wang, X. Yuan, B. Zhang, H. Y. Chen and Q. S. Zheng, *Eur*. *J*. *Pharm*., 2010, **643**, 211-217.

[9] J. Xiong, J. B. Ni, G. Y. Hu, J. Shen, Y. Zhao, L. J. Yang, J. Q. Shen, G. J. Yin, C. Y. Chen, G. Yu, Y. L. Hu, M. Xing, R. Wan and X. P. Wang, *J. Ethnopharmacol*., 2013, **145**, 573-580.

[10] H. Y. Lee, S. M. Bae, K. J. Kim, W. Y. Kim, S. I. Chung, Y. Yang and Y. S. Yoon, *Life Sci*., 2011, **88**, 294-301.

[11] H. Wu, J. S. Xie, Q. R. Pan, B. B. Wang, D. Q. Hu and X. Hu, *PLOS ONE*, 2013, **8**: e52706.
[12] K. Nadine and R.Beate, *J. Nat. Prod.*, 2012, **75**, 865-869.
[13] H. Y. Lin, W. Chen, J. Shi, W. Y. Kong, J. L. Qi, X. M. Wang and Y. H. Yang, *Chem. Biol. Drug Des.*, 2013, **81**, 275-283.
[14] S. J. Lee, H. Sakurai, K. Koizumi, G. Y. Song, Y. S. Bae, H. M. Kim, K. S. Kang, Y. J. Surh, I. Saiki and S. H. Kim, *Cancer Lett.*, 2006; **233**: 57-67.
[15] W. Zhou, X. Zhang, L. Xiao, J. Ding, Q. H. Liu and S. S. Li, *Eur. J. Med. Chem.*, 2011, **46**, 3420-3427.
[16] W. Zhou, Y. Peng and S. S. Li, *Eur. J. Med. Chem.*, 2010, **45**, 6005-6011.
[17] S. H. Kim, I. C. Kang, T. J. Yoon, Y. M. Park, K. S. Kang, G. Y. Song, B. Z. Ahn, *Cancer Lett.*, 2001, **172**, 171-175.
[18] W. J. Wang, M. Dai, C. H. Zhu, J. G. Zhang, L. P. Lin, J. Ding and W. H. Duan, *Bioorg. Med. Chem. Lett.*, 2009, **19**, 735-737.
[19] Y. Tanoue, A. Terada and Y. Sugyö, *J. Org. Chem.*, 1987, **52**, 1437-1439.
[20] Q. Lu, W. J. Liu, J. Ding and J. C. Cai, *Bioorg. Med. Chem. Lett.*, 2002, **12**, 1375-1378.
[21] F. Yang, Y. Chen, W. H. Duan, C. Zhang, H. Zhu and J. Ding, *Int. J. Cancer*, 2006, **119**, 1184-1193.
[22] Y. H. Su, J. S. Xie, Y. G. Wang, X. Hu and X. F. Lin, *Eur. J. Med. Chem.*, 2010, **45**, 2713-2718.
[23] Z. S. Huang, H. Q. Wu, Z. F. Duan, B. F. Xie, Z. C. Liu, G. K. Feng, L. Q. Gu, A. S. C. Chan and Y. M. Li, *Eur. J. Med. Chem.*, 2004, **39**, 755-764.
[24] R. Deng, J. Tang, B. F. Xie, G. K. Feng, Y. H. Huang, Z. C. Liu and X. F. Zhu, *Int. J. Cancer*, 2010, **127**, 220-229.
[25] B. Ernst and J. L. Magnani, *Nat. Rev. Drug. Discov.*, 2009, **8**, 661-677.
[26] Y. Ikehara, T. Niwa, L. Biao, S. K. Ikehara, N. Ohashi, T. Kobayashi, Y. Shimizu, N. Kojima and H. Nakanishi, *Cancer Res*, 2006, **66**, 8740-8748.
[27] T. Ohgami, K. Kato, H. Kobayashi, K. Sonoda, T. Inoue, S. Yamaguchi, T. Yoneda and N. Wake, *Cancer Sci.*, 2010, **101**, 1387-1395.
[28] H. He, L. P. Bai and Z. H. Jiang, *Bioorg. Med. Chem. Lett.*, 2012, **22**, 1582-1586.
[29] J. M. Langenhan, N. R. Peters, I. A. Guzei, F. M. Hoffmann and J. S. Thorson, *PNAS*, 2005, **102**, 12305-12310.
[30] L. M. Zhao, T. P. Xie, Y. Q. He, D. F. Xu and S. S. Li, *Eur. J. Med. Chem.*, 2009, **44**, 1410-1414.
[31] B. S. Furniss, A. J. Hannaford, P. W. G. Smith and A.R. Tatchell, *Textbook of Practical Organic Chemistry*, 1989, p. 647-648.
[32] M. M. Ponpipom and R. L. Bugianesi, *J. Med. Chem.*, 1987, **30**, 136-142.
[33] S. W. Wang, S. L. Pan, Y. C. Huang, J. H. Guh, P. C. Chiang, D. Y. Huang, S. C. Kuo, K. H. Lee and C. M. Teng, *Mol. Cancer Ther*. 2008, **7**, 350-360.
[34] R. Huey, G. M. Morris, A. J. Olson and D. S. Goodsell, *J. Comput. Chem.*, 2007, **28**, 1145-1152.

Figure and table captions:

Fig. 1 Chemical structures of compound **A-I**.

Fig. 2 Molecular docking analysis of **IIb**, showing proposed binding modes at the colchicine binding pocket *β*-tubulin (PDB code: 1SA0). Hydrogen bonds are displayed as lime dashed lines. (A) and (C) Interaction of **IIb** with the amino acid residues of colchicine binding site (carbon atom, gray; oxygen atom, red; hydrogen atom, white; sulphur atom, yellow). (B) and (D) Binding pose of **IIb** in the protein surface of tubulin (carbon atom, green; oxygen atom, red; hydrogen atom, white; sulphur atom, yellow and nitrogen atom; light blue).

Fig. 3 Effect of **IIb** on the cell cycle distribution of HepG2 cells. (A) Cells treated with 0, 3 and 10 μM **IIb** for 24 hours were collected and processed for analysis. (B) Cells treated with 3 μM **IIb** for different time was collected and analyzed.

Fig. 4 AnnexinV/PI dual-immuno- fluorescence staining after treatment with different concentrations of **IIb** for different time revealed significantly increased number of apoptotic and necrotic cells (measured with Annexin V+/PI+ cells). (A) Cells treated with 0, 0.3, 1 and 3 μM **IIb** for 24 hours were collected and processed for analysis. (B) Cells treated with 3 μM **IIb** for different time (0 h, 12 h, 24 h and 48 h) was collected and analyzed. The percentage of early apoptotic cells in the lower right quadrant (annexin V-FITC positive/PI negative cells), as well as late apoptotic cells located in the upper right quadrant (annexin V-FITC positive/PI positive cells).

Fig. 5 Effect of **IIb** (3 μM) on interphase microtubules of HepG2 cells. Microtubules tagged with rhodamine (red) and nuclei tagged with DAPI (blue) were observed under a confocal microscope.

Fig. 6 IIb affected microtubule assembly *in vitro*. After 24 hours treatment with **IIb** (3 μM), paclitaxel (1 μM) and colchicine (1 μM), cytosolic (S, soluble) and cytoskeletal (P, polymerized tubulin) tubulin fractions were separated and immunoblotted with antibody against *β*-tubulin.

Scheme 1 Regents and conditions: a) Etanol, nitrogen, room temperature, 30 minutes; b) Etanol, nitrogen, room temperature to 0 °C, 30 minutes; c) Etanol, nitrogen, room temperature to 60 °C, 1 hour.

Table 1 Inhibition of tubulin polymerization and cell proliferation against MG63, MCF-7, B16-F10, HepG2, MDA-231, L02, VERO and MCF-10A cells by **Ia-IIId**

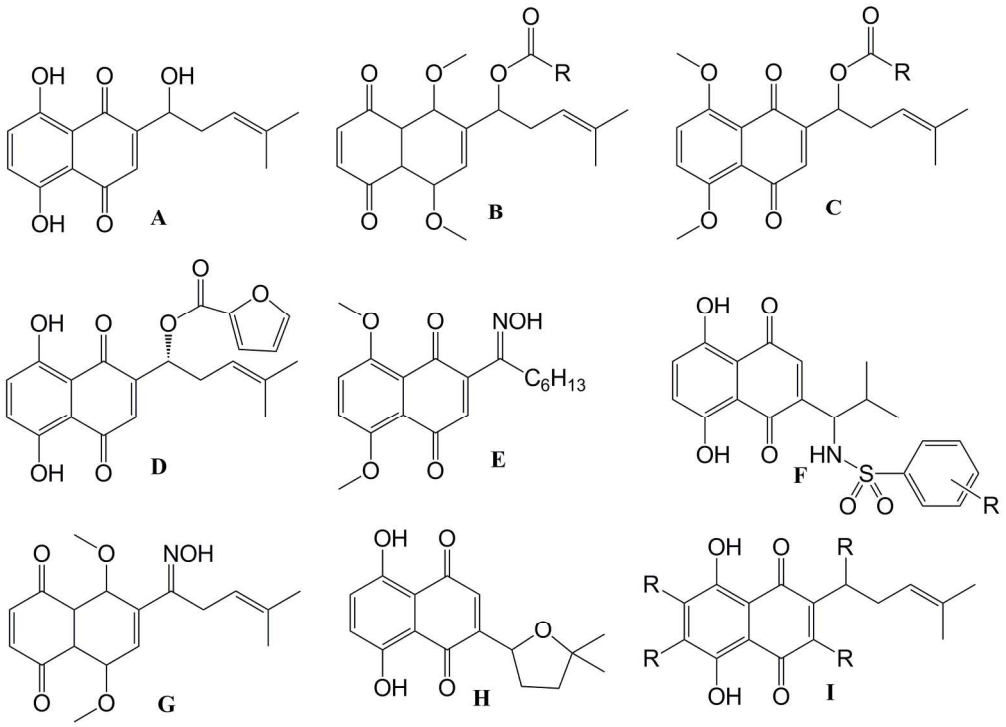

Fig. 1 Chemical structures of compound A-I.
183x132mm (300 x 300 DPI)

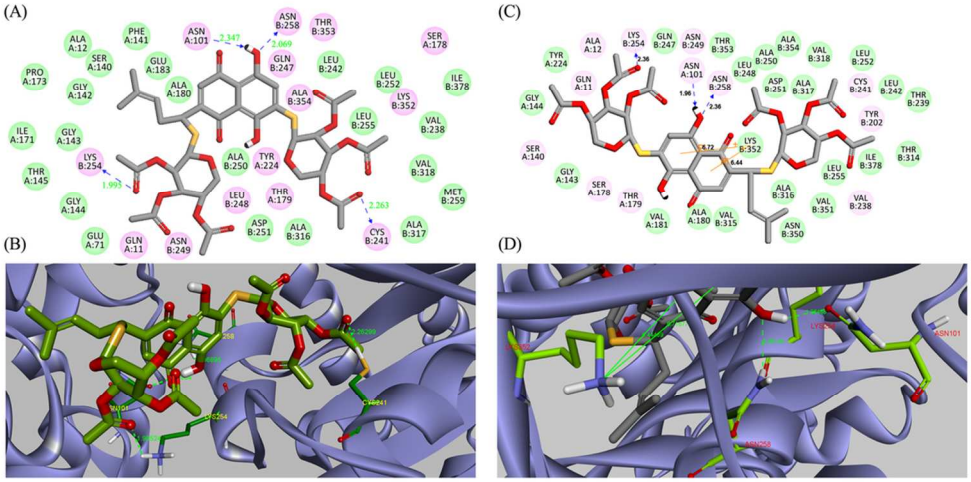

Fig. 2 Molecular docking analysis of IIb, showing proposed binding modes at the colchicine binding pocket β-tubulin (PDB code: 1SA0). Hydrogen bonds are displayed as lime dashed lines. (A) and (C) Interaction of IIb with the amino acid residues of colchicine binding site (carbon atom, gray; oxygen atom, red; hydrogen atom, white; sulphur atom, yellow). (B) and (D) Binding pose of IIb in the protein surface of tubulin (carbon atom, green; oxygen atom, red; hydrogen atom, white; sulphur atom, yellow and nitrogen atom; light blue).
101x51mm (300 x 300 DPI)

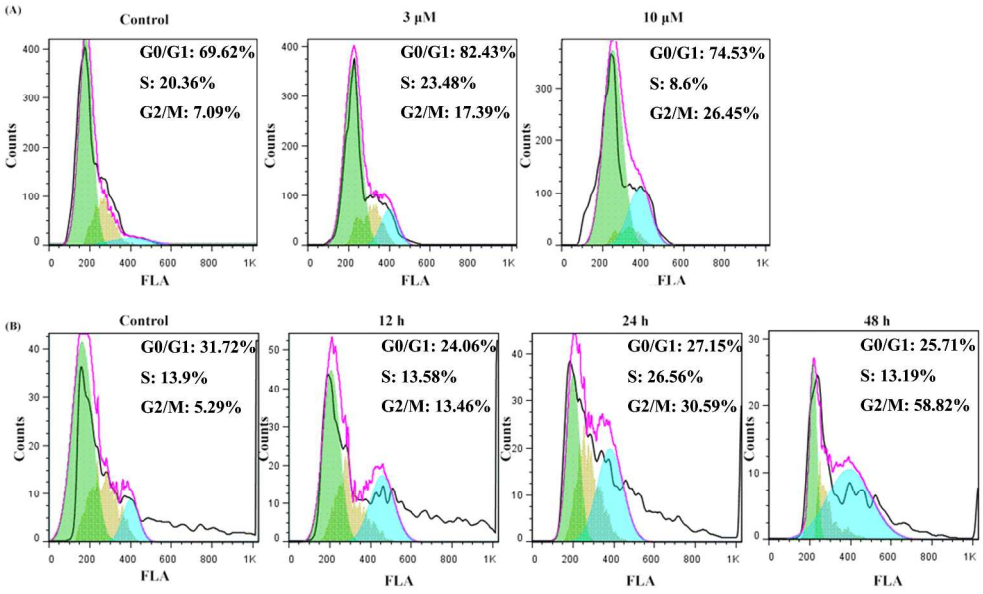

Fig. 3 Effect of IIb on the cell cycle distribution of HepG2 cells. (A) Cells treated with 0, 3 and 10 μM IIb for 24 hours were collected and processed for analysis. (B) Cells treated with 3 μM IIb for different time was collected and analyzed.
365x217mm (300 x 300 DPI)

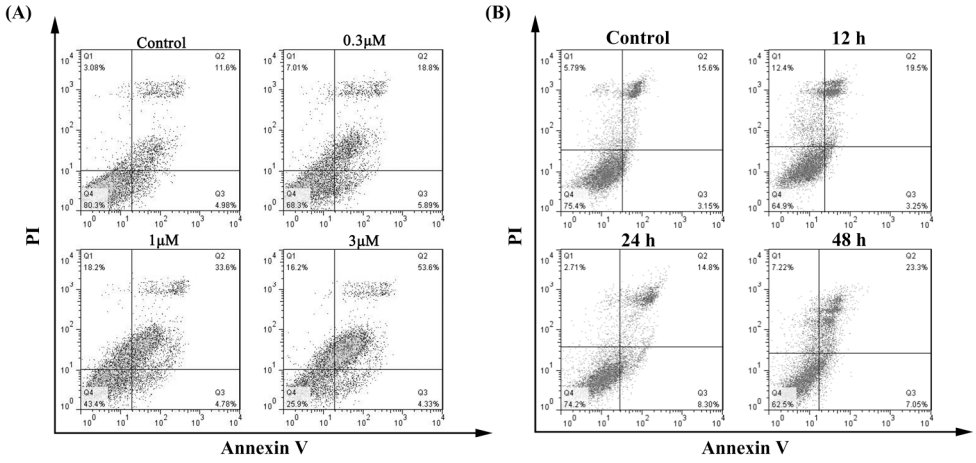

Fig. 4 AnnexinV/PI dual-immuno- fluorescence staining after treatment with different concentrations of IIb for different time revealed significantly increased number of apoptotic and necrotic cells (measured with Annexin V+/PI+ cells). (A) Cells treated with 0, 0.3, 1 and 3 μM IIb for 24 hours were collected and processed for analysis. (B) Cells treated with 3 μM IIb for different time (0 h, 12 h, 24 h and 48 h) was collected and analyzed. The percentage of early apoptotic cells in the lower right quadrant (annexin V-FITC positive/PI negative cells), as well as late apoptotic cells located in the upper right quadrant (annexin V-FITC positive/PI positive cells).
211x105mm (300 x 300 DPI)

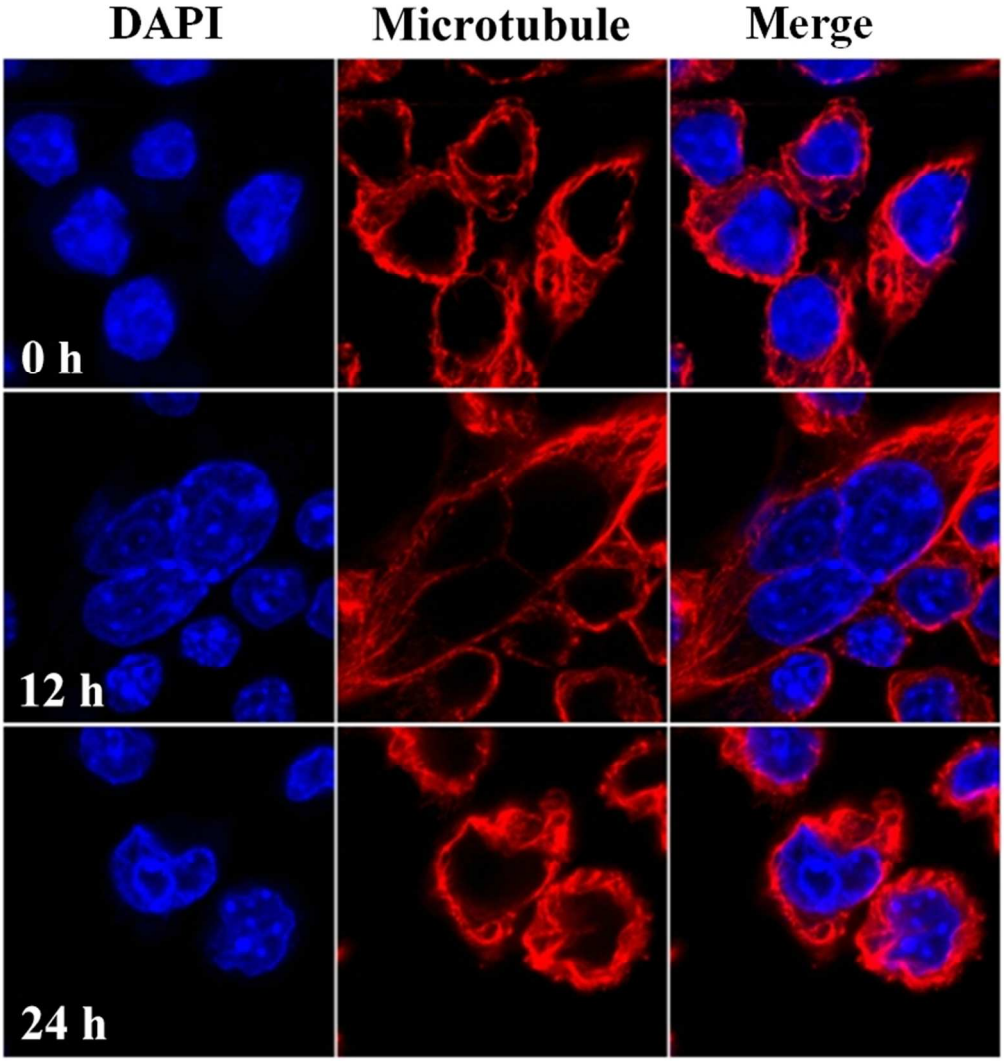

Fig. 5 Effect of IIb (3 μM) on interphase microtubules of HepG2 cells. Microtubules tagged with rhodamine (red) and nuclei tagged with DAPI (blue) were observed under a confocal microscope.
139x151mm (150 x 150 DPI)

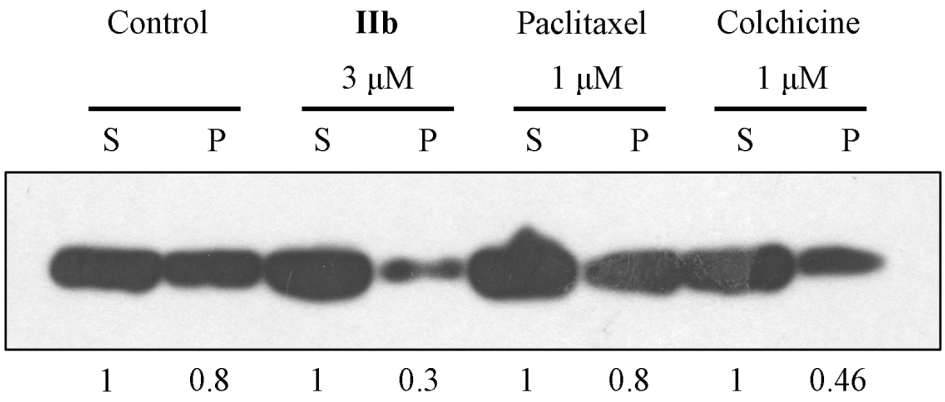

Fig. 6 IIb affected microtubule assembly in vitro. After 24 hours treatment with IIb (3 μM), paclitaxel (1 μM) and colchicine (1 μM), cytosolic (S, soluble) and cytoskeletal (P, polymerized tubulin) tubulin fractions were separated and immunoblotted with antibody against β-tubulin.
149x63mm (300 x 300 DPI)

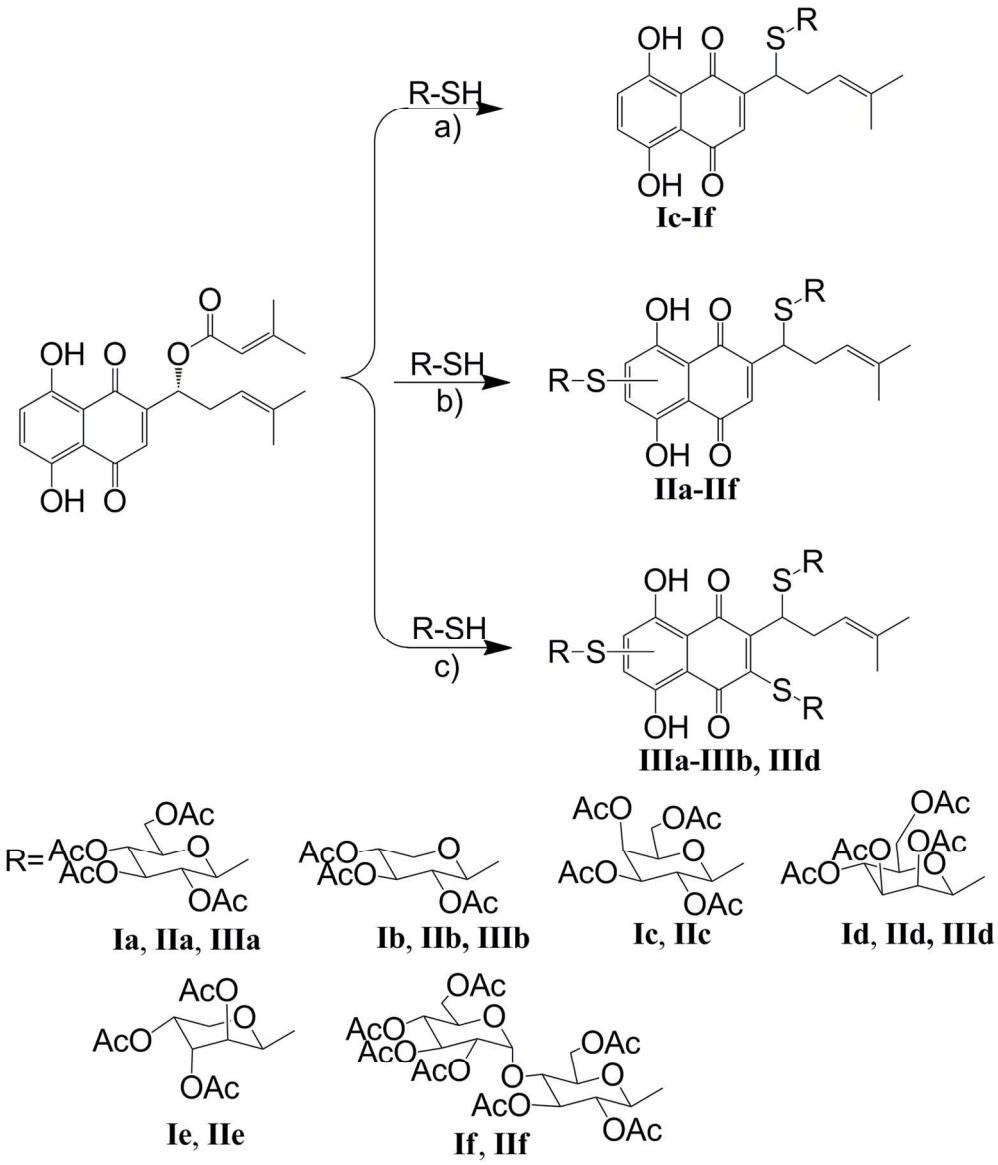

Scheme 1 Regents and conditions: a) Etanol, nitrogen, room temperature, 30 minutes; b) Etanol, nitrogen, room temperature to 0 °C, 30 minutes; c) Etanol, nitrogen, room temperature to 60 °C, 1 hour.
137x159mm (300 x 300 DPI)

Table 1 Inhibition of tubulin polymerization and cell proliferation against MG63, MCF-7, B16-F10, HepG2, MDA-231, L02, VERO and MCF-10A cells by **Ia**–**IIId**

Compt	IC_{50} (μM)								
	MG63[a]	MCF-7[a]	B16-F10[a]	HepG2[a]	MDA-231[a]	L02[a]	VERO[a]	MCF-10A[a]	Tubulin[b]
Ia	4.37±0.231	4.75±0.255	7.07±0.363	85.9±2.73	62.3±1.56	134±4.68	83.3±2.04	121±4.96	10.0±0.311
IIa	2.61±0.165	6.30±0.344	3.98±0.276	99.7±3.44	49.8±1.25	122±4.05	87.9±2.16	90.5±3.56	18.5±1.47
IIIa	3.99±0.372	7.84±1.23	4.62±0.698	91.5±3.02	96.7±2.99	107±3.98	93.1±2,98	120±4.21	14.0±1.69
Ib	9.16±0.640	29.7±1.66	14.1±0.786	98.3±3.46	137±4.49	125±3.48	84.8±2.56	132±4.68	41.2±1.79
IIb	1.22±0.221	2.37±0.165	4.53±0.247	1.22±0.110	10.6±0.97	132±4.71	82.5±2.00	78.1±2.27	4.67±0.433
IIIb	1.38±0.178	3.13±0.342	3.75±0.273	89.1±2.98	47.9±1.04	146±4.89	99.7±3.27	70.1±2.08	7.57±0.742
Ic	4.67±0.127	14.5±0.862	6.88±0.293	98.9±3.06	4.97±0.37	88.2±2.37	78.5±1.77	87.2±2.28	32.8±1.98
IIc	3.58±0.63	15.3±1.03	6.26±0.970	82.4±2.06	93.2±3.01	73.8±2.21	99.7±3.05	94.5±2.26	28.1±2.01
Id	3.20±0.212	6.67±0.423	9.24±0.524	-	-	-	-	-	18.0±1.02
IId	2.71±0.0924	12.2±1.01	11.6±1.29	76.0±1.99	94.6±2.99	89.1±2.79	96.3±2.27	42.5±1.88	40.8±2.98
IIId	4.47±0.148	7.97±0.991	5.93±0.571	97.9±3.08	76.5±2.96	95.3±3.44	85.5±2.21	92.3±2.69	17.3±2.23
Ie	15.58±1.84	24.3±1.913	14.2±0.553	94.6±2.97	81.8±2.34	95.2±3.35	74.2±1.88	95.3±3.07	53.8±2.35
IIe	11.06±0.913	10.28±0.873	11.4±0.980	97.2±2.11	78.5±2.01	90.9±3.10	77.6±2.03	113±4.42	26.4±1.09
If	3.34±0.115	11.2±0.830	9.72±0.475	95.1±2.84	67.3±1.94	81.2±2.55	71.6±1.99	91.5±2.99	31.1±1.88
IIf	2.63±0.267	10.0±0.871	6.79±0.856	78.3±2.00	69.8±1.88	126±4.85	30.5±1.45	58.8±1.57	13.2±1.04
Shikonin	7.36±0.374	23.6±1.21	17.9±0.895	2.73±0.286	108±4.89	83.8±2.07	6.76±0.684	93.4±3.37	16.8±0.625
Colchicine	-	-	-	-	-	-	-	-	3.83±0.424

[a] Inhibition of the growth of tumor cell lines.

[b] Inhibition of tubulin polymerization.

- Not determined.